Analysis of minimal and maximal pressures, uncertainty and spectral density of fluctuating pressures beneath classical hydraulic jumps

Seyed Nasrollah Mousavi, Davood Farsadizadeh, Farzin Salmasi, Ali Hosseinzadeh Dalir and Daniele Bocchiola

ABSTRACT

Knowledge of extreme pressures and fluctuations within stilling basins is of the utmost importance, as they may cause potential severe damages. It is complicated to measure the fluctuating pressures of hydraulic jumps in real-scale structures. Therefore, little information is available about the pressure fluctuations in the literature. In this paper, minimal and maximal pressures were analyzed on the flat bed of a stilling basin downstream of an Ogee spillway. Attention has been focused on dimensionless pressures related to the low and high cumulative probabilities of occurrence ($P^*_{0.1\%}$ and $P^*_{99.9\%}$), respectively. The results were presented based on the laboratory-scale experiments. These parameters for the relatively high Froude numbers have not been investigated. The total standard uncertainty for the dimensionless mean pressures (P^*_m) was obtained around 1.87%. Spectral density analysis showed that the dominant frequency in the classical hydraulic jumps was about 4 HZ. Low-frequency of pressure fluctuations indicated the existence of large-scale vortices. In the zone near the spillway toe, $P^*_{0.1\%}$ reached negative values of around −0.3. The maximum values of pressure coefficients, namely $|C_{P0.1\%}|_{max}$ and $C_{P99.9\%max}$, were achieved around 0.19 and 0.24, respectively. New original expressions were proposed for $P^*_{0.1\%}$ and $P^*_{99.9\%}$, which are useful for estimating extreme pressures.

Key words | classical hydraulic jump, cumulative probabilities of occurrence, minimal and maximal pressures, pressure coefficients, spectral density analysis, total standard uncertainty

HIGHLIGHTS

- Analysis of the minimal and maximal values of pressures ($P^*_{0.1\%}$ and $P^*_{99.9\%}$).
- Investigation of the longitudinal distribution of dimensionless pressure coefficients along the hydraulic jumps ($C_{P0.1\%}$, $C_{P99.9\%}$ and C'_P).
- Evaluation of the power spectral density (PSD) analysis to determine the dominant frequency of fluctuating pressures in the classical hydraulic jumps.
- Calculation of the total standard uncertainty for the multiple variables ($P^*_{0.1\%}$, $P^*_{99.9\%}$, P^*_m, $C_{P0.1\%}$ and $C_{P99.9\%}$).
- Propose new original best-fit relationships to estimate the dimensionless extreme pressure data ($P^*_{0.1\%}$ and $P^*_{99.9\%}$).

Seyed Nasrollah Mousavi
Davood Farsadizadeh (corresponding author)
Farzin Salmasi
Ali Hosseinzadeh Dalir
Department of Water Engineering,
University of Tabriz,
Tabriz 5166616471,
Iran
E-mail: *farsadi@tabrizu.ac.ir*

Daniele Bocchiola
Department of Civil and Environmental Engineering (DICA),
Politecnico di Milano,
L. da Vinci, 32, Milano 20133,
Italy

doi: 10.2166/ws.2020.098

INTRODUCTION

Hydraulic jump has many applications in the field of hydraulics, including energy dissipation, protection of structures downstream of spillways, rapid mixing of chemicals for wastewater treatment, flow aeration, and de-chlorination. This phenomenon usually occurs inside the stilling basins to establish the flow with the appropriate energy at the downstream of the structure (Macián-Pérez *et al.* 2020). Based on the range of the values of incident Froude number (Fr_1), there are two common types of hydraulic. The most effective hydraulic jump occurs in the range of $4.5 < Fr_1 < 10$, which reduces the length of stilling basins (Chanson & Carvalho 2015).

Distribution of mean pressures in hydraulic jumps has been widely investigated in the literature. In turbulent flows, the fluctuating pressure and velocity may be more important than the mean values. Evaluation of pressures on the basin bed is required to optimize the slab thickness. To analyze the forces affecting the stability of the stilling basin slab, it is necessary to determine the minimal and maximal pressures.

Macro-turbulence in hydraulic jumps produces large pressure fluctuations on the bed and walls of the stilling basins. This may cause severe damage, due to the lifting of the floor slab, erosion of materials, and cavitation (Toso & Bowers 1988), also potentially including the effect on seepage (Fiorotto & Caroni 2014). It is very difficult to measure the fluctuating pressures of hydraulic jumps in the field. Therefore, little information is available on pressure fluctuations in the literature (Onitsuka *et al.* 2007). It is necessary to perform experiments of pressure fluctuations in the laboratory-scale structures (Farhoudi *et al.* 2010). Since turbulent pressure patterns are random, much has been done to define some of the statistical parameters (Toso & Bowers 1988). Indeed, the United States Bureau of Reclamation (USBR) provides general design criteria for stilling basins, concerning basin length and sequent depths. However, no indications are given about possible different jump types, pressure regimes, and forces on the basin (Padulano *et al.* 2017).

Endres (1990) investigated the intensity coefficient of pressure fluctuations (C'_P), with different results from those obtained by Vasiliev & Bukreyev (1967) and Abdul-Khader & Elango (1974). The difference in the data was probably related to the degree of flow boundary layer development. Souza *et al.* (2015) compared the values of mean pressures, pressure fluctuations, and the data obtained by others. The results showed that the distribution of pressure fluctuations and mean pressures tends to behave similarly to those of the other authors. However, these values tended to be higher than those obtained by Endres (1990), Marques *et al.* (1997), Pinheiro (1995) and followed the development of Daí Prá (2011). This difference was related to the determination of Y_1, Y_2, the initial position of the hydraulic jump, and the submergence influence. Dai Prá *et al.* (2016) evaluated the hydrodynamic effects of flow conditions that affect the hydraulic jumps. These effects include the transition from the vertical curve between the spillway toe and stilling basin, the supercritical flow in a smooth basin, and the macro-turbulence characteristics of free and submerged hydraulic jumps. Novakoski *et al.* (2017) studied bed pressures downstream of a stepped spillway. A significant difference was found at the beginning of the stilling basin, with the 99.9% cumulative probability of occurrence. They concluded that this difference might be due to the absence of a toe curve between the stepped spillway and stilling basin. Chiew & Emadzadeh (2017) showed that the mean pressure calculated from the pressure fluctuations is less than that obtained from the water surface profile using high-speed images. Based on the estimation method proposed by Teixeira (2003), Hampe *et al.* (2020) evaluated the extreme pressures for the flat bed of a stilling basin downstream of a spillway, in the case of its application for the low Froude numbers ($Fr_1 \leq 4.5$).

Some cases of damage in stilling basins due to turbulent flow were presented in the report of ICOLD (Sánchez Bribiesca & Vizcaíno 1973). For instance, damage to the stilling basin of the Malpaso-Mexico dam occurred during the passage of a 3000 m^3/s flow discharge in 1970 and caused the lifting of 720-ton of the basin slab. Also, there are two cases in which the macro-turbulence generated by a hydraulic jump caused damage or need to repair in stilling basins, Karnafuli Hydroelectric Power Plant Project, Bangladesh (1961) and Scofield Dam, Utah, USA (2005) (Alves 2008).

Determination of the C'_P coefficient is not enough for cavitation tendency analysis or slab lift action calculation (Lopardo *et al.* 2004). The work aims to measure the extreme pressures related to the low and high cumulative probabilities of occurrence ($P^*_{0.1\%}$ and $P^*_{99.9\%}$). This study deals with the analysis of the values of $P^*_{0.1\%}$ and $P^*_{99.9\%}$ for different incident Froude numbers (Fr_1) with relatively high values (7.12 to 9.46) along the free hydraulic jumps. For reference, the results were compared with the data obtained by others. The power spectral density (PSD) of measured fluctuating pressure data was analyzed to determine the dominant frequency of random processes. In addition, the total standard uncertainty for the measured and multiple variables along the stilling basin was evaluated. Also, the probability density function (PDF) for the fluctuating pressures was plotted at different pressure taps. The distribution of dimensionless pressure coefficients was investigated along the hydraulic jumps. For technical purposes, new original best-fit relationships were developed to estimate the parameters of $P^*_{0.1\%}$ and $P^*_{99.9\%}$.

The manuscript is organized as follows. First, the materials used, and the methods adopted in the laboratory-scale experimental study are reported. Then, the main results in terms of the statistics of the pressure field along the basin will be presented. Afterward, findings concerning the present literature will be discussed. Finally, some conclusions are provided and ways forward.

MATERIALS AND METHODS

Experimental setup and instruments

The case of a hydraulic jump in a flat and horizontal rectangular channel is well known as the classical hydraulic jump (CHJ) (Valero *et al.* 2019). Experiments were carried out in the hydraulic laboratory at the University of Tabriz, Iran (Figure 1). An experimental setup consisted of a stilling basin with 200 cm length (L_b) in a horizontal flume. The flume has a width of 51 cm, a height of 60 cm, and an approximate length of 10 m. An Ogee spillway with 70 cm height (H) was designed according to USBR recommendations (USBR 1987; Chanson & Carvalho 2015).

According to Figure 1, the subcritical depth (Y_2) was measured using an ultrasonic sensor of Datalogic with the US30 series and PR–5–N13–VH model, made in Italy. The operating distance (typical values) of this sensor is 100 to 1000 mm, with the minimum resolution of 1 mm. The Y_2 parameter was measured at the endpoint of the hydraulic jump length (L_j). As a result, all air bubbles have been removed, and the uniform flow was established along the flume. The values of the supercritical depth (Y_1) were calculated using the continuity equation. The mean incident velocity (V_1) was calculated as follows (Peterka 1984):

$$V_1 = \sqrt{2g \times \left(H + \frac{d_0}{2}\right)} \quad (1)$$

where d_0 is the hydraulic head upstream of the spillway crest, and g is the gravitational acceleration. The flow discharge (Q) was measured using a portable transit-time ultrasonic flowmeter with an accuracy of ±1%. Experiments were carried out with different incident Froude numbers (Fr_1), as summarized in Table 1. To measure the time series of instantaneous pressures, 25 pressure taps were considered on the bed of the stilling basin (Figure 2).

Pressure transducers were selected to be Atek BCT 110 series with 100 mbar-A-G1/4 model, made in Turkey. The six transducers were mounted at different points along the stilling basin. The measuring range is from −100 to 100 cm, with an accuracy of ±0.5%. Figure 1(a) shows that pressure transducers were mounted on a support plate and connected to the flexible hoses. An important point in using a transducer instrument is that it should be at the same level as the basin bed. As a result, the measured pressures will be equal to the pressures on the bed of the stilling basin. The transparent plastic hoses with an internal diameter of 3 mm were connected to the pressure taps with the screws and positioned under the bottom of the flume. Due to the laboratory conditions, the maximum length of hoses was considered to be 200 cm for the pressure taps at the end of the basin. Therefore, for the first part of the hydraulic jump, which is very important, it has been tried as much as possible to use the minimum hose length to connect the transducer to the pressure tap. Under these conditions, the effect of the hose on data quality is minimized.

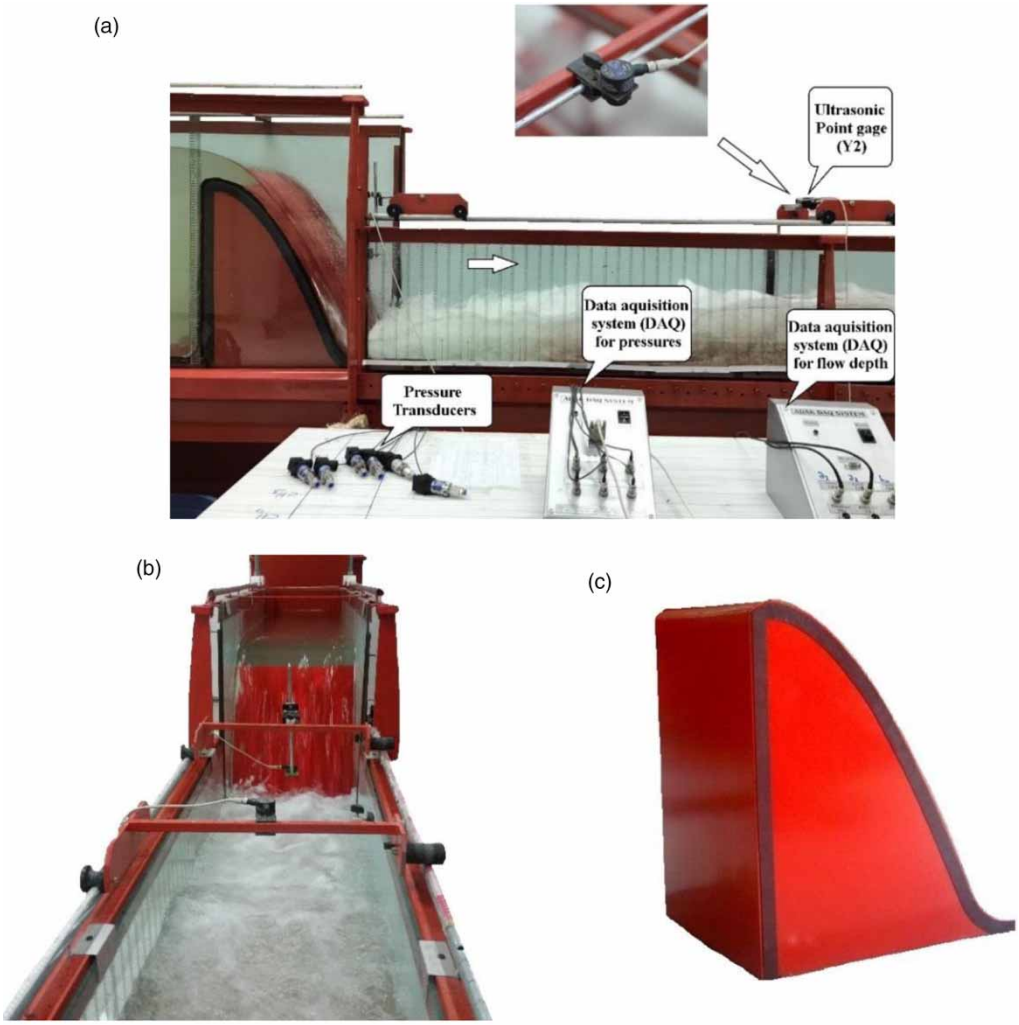

Figure 1 | Laboratory flume with the experimental setup: (a) details of measuring instruments, (b) downstream view of the spillway, and (c) view of the spillway.

Table 1 | Experimental parameters along the hydraulic jump

Fr_1	Q (L/s)	d_0 (cm)	Y_1 (cm)	Y_2 (cm)	V_1 (m/s)	L_j (cm)
7.12	60.4	14.39	3.04	27.55	3.89	189.0
7.44	55.0	13.77	2.78	26.84	3.88	189.0
7.59	52.7	13.35	2.66	26.05	3.88	189.0
7.96	47.5	12.52	2.41	24.87	3.87	189.0
8.34	43.0	12.02	2.18	23.70	3.86	162.5
9.46	33.0	10.65	1.68	20.65	3.84	142.5

There was significant air entrainment in the upstream part of the hydraulic jump (Figure 1(b)). There should be no air bubbles along the hoses to alleviate the influence of air on the pressure transducers. The hoses should not be made of soft or hard material so that they can transmit the correct values of pressures to the transducers and can be easily used. To do this, for all experiments, hoses should be de-aerated by establishing a uniform flow within the flume before the hydraulic jump formation. The hoses de-aeration depends on experience. In the present study, this important issue was carried out with the utmost attention and effort using the small valves installed at the end of the hoses. After ensuring that the entire length of the hoses was fully de-aerated, they were connected to the transducers. If there is any air bubble along the hose, it should be moved out of the hose by slightly opening the valve at the end of the hose. As a result, the acquisition of pressure data was acceptable.

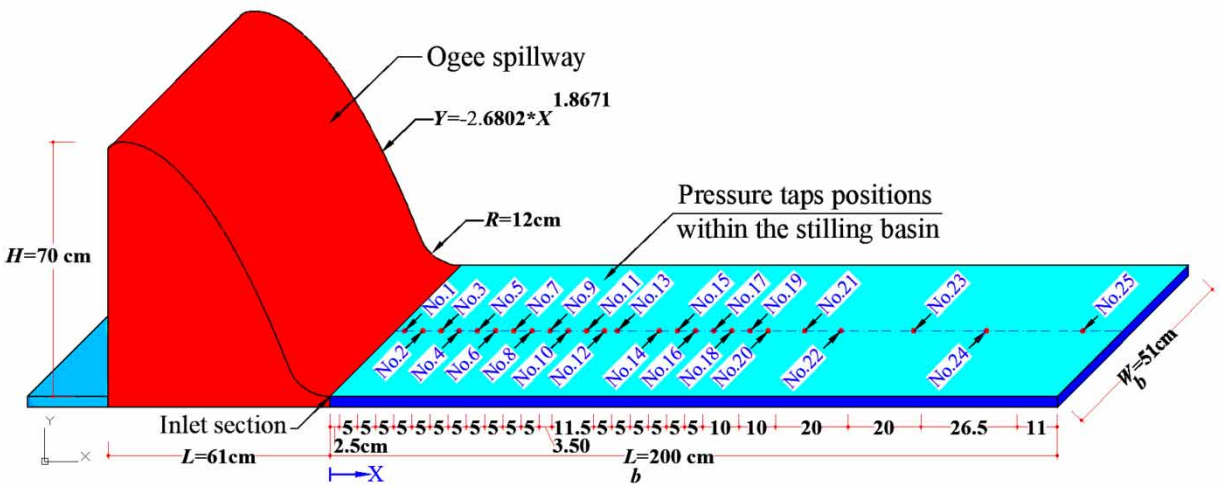

Figure 2 | Schematic view of the experimental setup, and the longitudinal distribution of pressure taps.

Statistical data analysis

The statistical data analysis includes the determination of pressure parameters (P^*_k) such as the mean pressure head (P_m) and the pressure head with a certain cumulative probability of occurrence ($P_{a\%}$). The values of $P_{a\%}$ were calculated using the probability distribution of the instantaneous pressures. Marques *et al.* (1997) proposed Equation (2) for the dimensionless pressure parameters (P^*_k), namely P^*_m and $P^*_{a\%}$.

$$P^*_k = \frac{P_k - Y_1}{Y_2 - Y_1} \tag{2}$$

In the present study, the parameter of hydraulic jump length (L_j) has been considered to normalize the position of the pressure taps ($X^* = X/L_j$), where X^* is the dimensionless distance of each point from the beginning of the stilling basin. It is necessary to determine the pressure coefficients in the design of the floor slab thickness. According to Equation (3), $C_{P(a\%)}$ is usually used as the dimensionless coefficient of pressure fluctuations with different cumulative probabilities of occurrence for the analysis of extreme pressures. The coefficients of $C_{P0.1\%}$ and $C_{P99.9\%}$ represent the maximum negative and positive pressure fluctuations relative to the mean pressure, as a function of the kinetic energy at the beginning of the hydraulic jump, respectively (Lopardo *et al.* 2004).

$$C_{P(a\%)} = \frac{P_{a\%} - P_m}{V_1^2/2g} \tag{3}$$

The results of Alves (2008) showed the longitudinal distribution of the $C_{P0.1\%}$ and $C_{P99.9\%}$ coefficients has a much smaller dispersion. As stated by Toso & Bowers (1988), pressure fluctuations related to 1% of the cumulative probability of occurrence do not lead to conservative pressure values. The dimensionless standard deviation of the pressure data series (σ_X) is known as the intensity coefficient of pressure fluctuations (C'_P), according to Equation (4) (Toso & Bowers 1988).

$$C'_P = \frac{\sigma_X}{V_1^2/2g} \tag{4}$$

The PDFs of fluctuating pressures for different pressure taps were plotted using EasyFit professional software (EasyFit 2010). $P^*(Z)$ is the probability density function of the normalized pressure level (Z) (Fiorotto & Rinaldo 1992).

$$Z(X, t) = \frac{P(X, t) - P_m}{\sigma_X} \tag{5}$$

$$P^*(Z) = \frac{1}{\sqrt{2\pi}} \times Exp\left(-\frac{Z^2}{2}\right) \tag{6}$$

where $P(X,t)$ is the instantaneous pressure of the sample data at each pressure tap. The dimensions of $P(X, t)$, P_m, and σ_X are in cm of column water.

Uncertainty analysis

The uncertainty due to the precision error ($S_{\overline{X}}$) is used for the errors that varied during the experiment. Also, the uncertainty due to the bias error (b_K) is related to the errors that were constant during the experiment. Based on the Taylor Series Method (TSM) (ISO 1993), the total uncertainty (u_X) is obtained using the root sum squares (RSS) of the combined elemental standard uncertainties (ASME 2013; Coleman & Steele 2018).

$$u_X = \left(S_{\overline{X}}^2 + \sum_{K=1}^{M} b_K^2 \right)^{\frac{1}{2}} \tag{7}$$

$$S_{\overline{X}} = \frac{S_X}{\sqrt{N}} \tag{8}$$

where S_X is the sample standard deviation of N measurements, and M is the number of bias error sources. The uncertainties of b_K are estimated in a variety of ways, such as the previous experience, manufacturer's specifications, and calibration data. The estimate of the bias error must be based on judgment. Using the TSM method, the dimensionless form of the total standard uncertainty (u_r/r) for the multiple variables of P^*_k (including P^*_m and $P^*_{a\%}$) and $C_{P(a\%)}$ would be appropriate in the uncertainty analysis. This leads to:

$$\left(\frac{u_{P_k^*}}{P_k^*}\right)^2 = \left(\frac{P_k}{P_k^*}\times\frac{\partial P_k^*}{\partial P_k}\right)^2 \times \left(\frac{u_{P_k}}{P_k}\right)^2 + \left(\frac{Y_2}{P_k^*}\times\frac{\partial P_k^*}{\partial Y_2}\right)^2 \times \left(\frac{u_{Y_2}}{Y_2}\right)^2 + \left(\frac{Z}{P_k^*}\times\frac{\partial P_k^*}{\partial Z}\right)^2 \times \left(\frac{u_Z}{Z}\right)^2 + \left(\frac{Q}{P_k^*}\times\frac{\partial P_k^*}{\partial Q}\right)^2 \times \left(\frac{u_Q}{Q}\right)^2 \tag{9}$$

$$\left(\frac{u_{C_{P(a\%)}}}{C_{P(a\%)}}\right)^2 = \left(\frac{P_{a\%}}{C_{P(a\%)}}\times\frac{\partial C_{P(a\%)}}{\partial P_{a\%}}\right)^2 \times \left(\frac{u_{P_{a\%}}}{P_{a\%}}\right)^2 + \left(\frac{P_m}{C_{P(a\%)}}\times\frac{\partial C_{P(a\%)}}{\partial P_m}\right)^2 \times \left(\frac{u_{P_m}}{P_m}\right)^2 + \left(\frac{Z}{C_{P(a\%)}}\times\frac{\partial C_{P(a\%)}}{\partial Z}\right)^2 \times \left(\frac{u_Z}{Z}\right)^2 \tag{10}$$

According to ISO (1993), the uncertainty at a certain level of confidence can be determined using an appropriate factor (k), as follows:

$$U_r = k_{\%}\, u_r \tag{11}$$

The large-sample assumption was considered for the uncertainty of the results at a 99% level of confidence ($U_{99} = 2.6{*}u$) (Coleman & Steele 2018). The average values of the total standard uncertainties at a 99% level of confidence for the measured and multiple variables are presented in Table 2.

RESULTS AND DISCUSSION

Power spectral density

In this section, the power spectral density (PSD) of the measured data at each pressure tap was analyzed using a MATLAB® code (MATLAB 2016) and the application of appropriate Fourier transform techniques. The PSD analysis is usually used to estimate the dominant frequency of random processes and indicates which frequency has substantial variations and vice versa. Figure 3(a) presents the experimental results of PSD at different pressure taps. Some of the points have one peak, and others have two peaks or more. There is a tendency for the peak frequencies to decrease as they move away from the beginning of the jump. This behavior was already verified by Neto & Marques (2008).

The results showed that in the classical hydraulic jumps, the highest PSD variations were related to the frequencies

Table 2 | Average values of the total standard uncertainties

Variable type	Symbol	U_X/X (%)	U_r/r (%)
Measured variables	Q	0.09	–
	Z	0.56	–
	Y_2	0.79	–
Multiple variables	Y_1	–	0.18
	Fr_1	–	0.23
	P^*_m	–	1.87
	$P^*_{0.1\%}$	–	1.25
	$P^*_{99.9\%}$	–	0.97
	$C_{P0.1\%}$	–	2.35
	$C_{P99.9\%}$	–	2.64

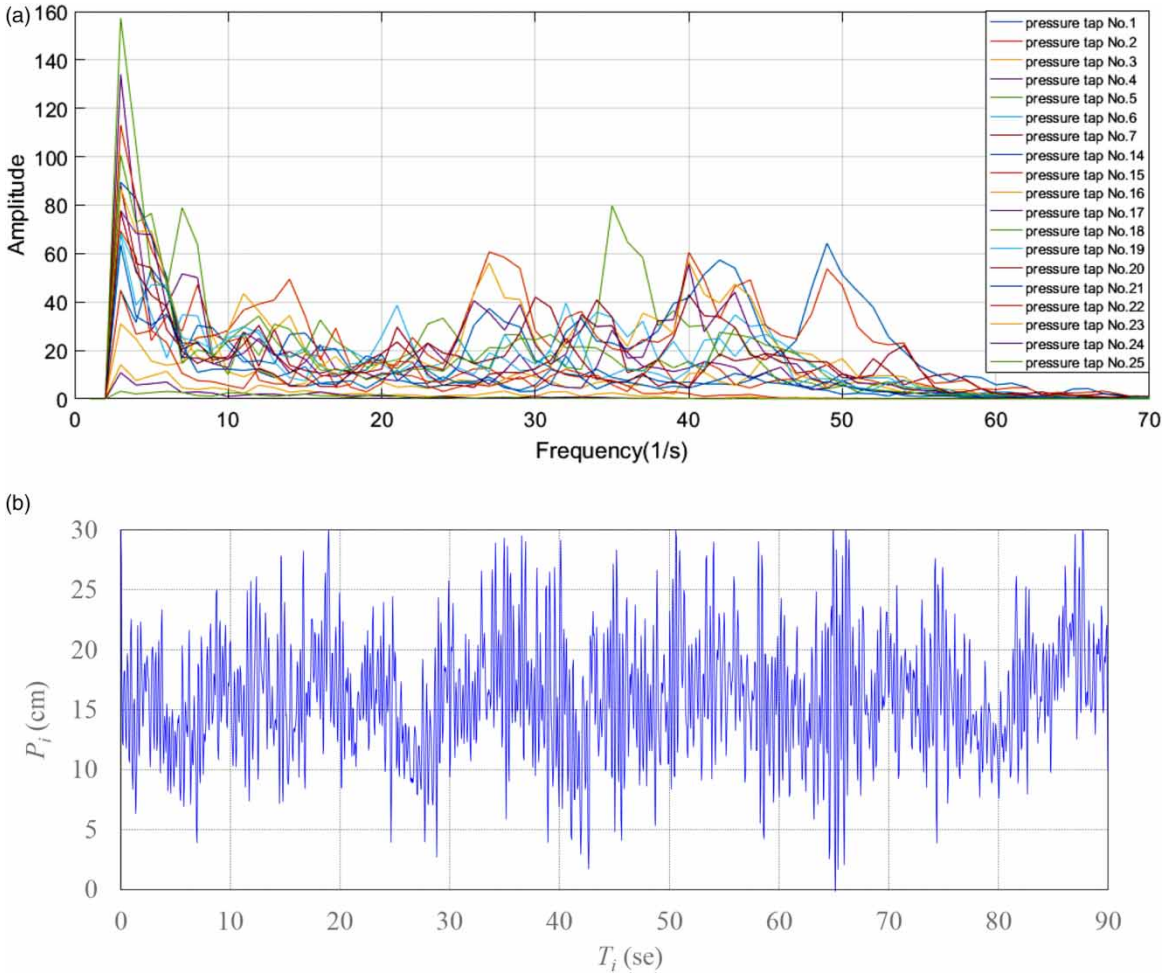

Figure 3 | Spectral analysis of pressure fluctuations beneath hydraulic jumps for $Fr_1 = 7.12$. (a) PSD function at different pressure taps. (b) Raw signal of the pressure transmitter at the pressure tap No. 9.

less than 5 Hz. According to sampling theory, the minimum frequency of data acquisition should be about twice the dominant frequency in the signal (Yan *et al.* 2006). Figure 3(a) shows that the maximum values of the vertical axis (amplitude) are close to the frequency of 4 Hz. Accordingly, the data acquisition frequency of 20 Hz with a duration of 90 seconds was used for each pressure tap. According to Pei-Qing & Ai-Hua (2007), large-scale eddies produce large and low-frequency pressure fluctuations and vice versa. This type of eddies carry on the main part of the turbulent energy and are called energy-carried eddies. Accordingly, hydraulic jumps can be considered as a rapidly varied flow with strong vortices that cause macro-turbulent fluctuations.

Figure 3(b) presents the time series diagram of the raw signals related to the pressure transducer at pressure tap No. 9, which has the maximum pressure fluctuations. It is observed that the turbulent pressures in hydraulic jumps are very stochastic. Accordingly, the application of statistical methods is necessary for the analysis of pressure data (Khatsuria 2005).

Probability density function

Figure 4 indicates that the PDFs at each pressure tap do not follow the normal distribution along the hydraulic jump, especially in the zone of $0 \leq X^* \leq 0.3$. In this zone, minimum and maximum extreme pressures ($P^*_{0.1\%}$ and $P^*_{99.9\%}$), have maximum differences with

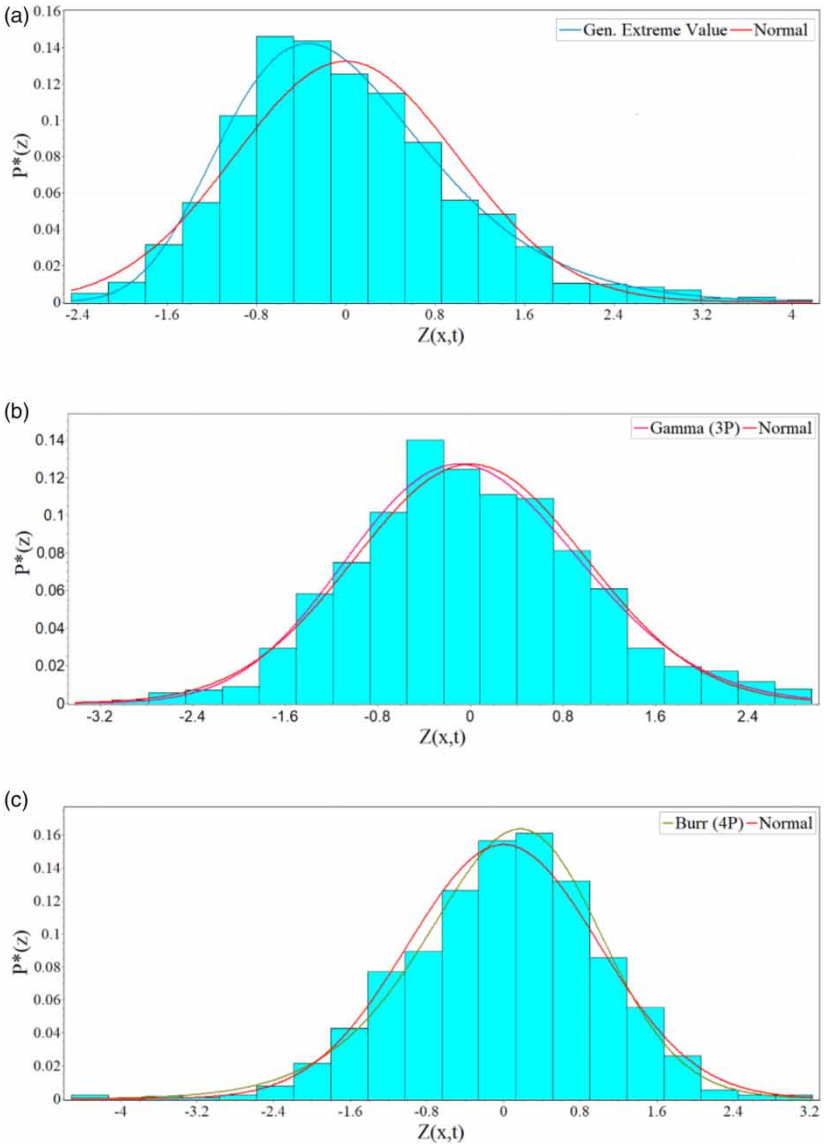

Figure 4 | Histogram of probability density function (a) Point 1, (b) Point 9, and (c) Point 25.

the mean pressures (P^*_m). In addition, the coefficients of skewness (S) and kurtosis (K) do not correspond to zero value. The skewness coefficient is a measure of the asymmetry of the data, indicating if the mean of the data is further out than the median. For a positive skewness, more values of instantaneous pressure data have fewer large values than the mean, and the tail is on the right side of the PDF distribution. For instance, Figure 4 presents the variations of $P^*(Z)$ as a function of $Z(X,t)$, compared with the normal distributions for different points along the stilling basin for $Fr_1 = 7.12$.

In accordance with the results of Fiorotto & Rinaldo (1992), at the beginning of the stilling basin, around the point 1 ($X^* = 0.013$), the positive pressure fluctuations are relatively more frequent than the negative pressure fluctuations ($S > 0$). At point 9, with the maximum pressure fluctuations ($X^*_{\sigma max} \approx 0.225$), the positive fluctuating pressures represent approximately the same frequency as the negative fluctuating pressures. Accordingly, at this position, the frequency distribution is normal ($S \approx 0$). Finally, at the endpoint of the jump, around the point 25 ($X^* = 1.00$), the skewness coefficient is negative. Therefore, negative

pressure fluctuations are more frequent than positive pressure fluctuations ($S < 0$).

Extreme pressures

As can be found in Figure 5, the extreme pressures increase with decreasing Froude number (i.e. increasing flow discharge) and cause an increase in the kinetic energy of the flow, and pressure fluctuations. This process indicates the intensity of flow turbulence along the hydraulic jump. The pressure values increase with an increment of the cumulative probability of occurrence, and the highest values of pressures corresponding to the highest cumulative probabilities of occurrence ($P^*_{99.9\%}$).

There are more fluctuations compared with the mean pressure at the positions close to the spillway toe (probably due to the incidence of flow in the stilling basin), reaching negative values around –0.3 up to the approximate $X^* \approx 0.3$. The negative values may indicate zones subject to low pressures, and may be related to erosion or cavitation processes. Beyond that, up to the position $X^* \approx 0.7$, the lowest values of pressures ($P^*_{0.1\%}$) have an ascending trend with a mild gradient. At the position $X^* \approx 1.0$, these data begin to oscillate near the dimensionless value of 1.0 and slightly lower. The $P^*_{99.9\%}$ data have higher and more different values compared with the mean values in the vicinity of the spillway toe, justified by the impact of flow on the stilling basin. The values of $P^*_{99.9\%}$ increase until $X^* \approx 0.3$. After that, up to the position $X^* \approx 0.7$, these values tend to decay almost linearly with a milder gradient, and then continue to decrease approximately until $X^* \approx 1.0$. It can be observed that the values of $P^*_{99.9\%}$ are nearly three times higher than the values of P^*_m at the position around $0.1 \leq X^* \leq 0.3$. The results seem to be in good agreement with Marques *et al.* (1997), along a stilling basin with a flat bed.

Proposition of relationships for the extreme pressures

Using the results obtained in the present study, by adjusting the dimensionless extreme pressure data ($P^*_{a\%}$), new second-order rational relationships were developed as a function of $0 \leq X^* \leq 1$. These relationships are valid for

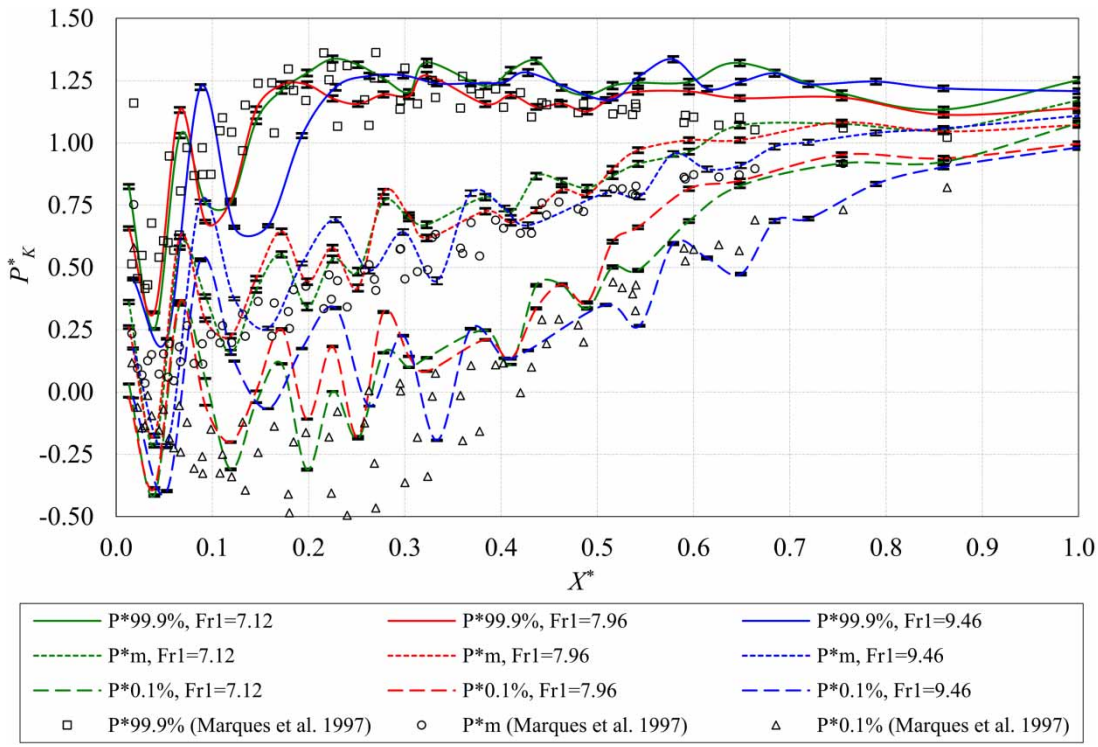

Figure 5 | Longitudinal distribution of $P^*_{0.1\%}$ and $P^*_{99.9\%}$, together with P^*_m with error bars.

the Froude numbers in the range of 7.12 to 9.46.

$$P^*_{a\%} = \frac{\alpha + \beta X^*}{1 + \gamma X^* + \delta X^{*2}} \quad (12)$$

The factors of α, β, γ, and δ are provided in Table 3. The accuracy of the relationships was assessed based on some statistical criteria, including determination coefficient (R^2), root mean squared error (RMSE), mean absolute error (MAE), and Willmott's Index of Agreement (WI) (Bennett *et al.* 2013). For a perfect fit, RMSE and MAE values are equal to zero, and WI values should be close to the unit. The obtained results are presented in Table 3.

Pressure coefficients

According to Figure 6, the values of $C_{P99.9\%}$, and C'_P coefficients rapidly increase in the region close to the spillway toe, until reaching the maximum values at the position around $0.10 \leq X^* \leq 0.30$. Afterward, these curves have a descending trend until they reach constant values. For the values of $C_{P0.1\%}$ coefficient, the variation trend at the beginning of the stilling basin is descending, until reaching the minimum values at the position around $0.10 \leq X^* \leq 0.30$. Afterward, the curves have an ascending trend until they reach constant values. The values of C'_P increase with decreasing Fr_1, which indicates that the flow turbulence is more intensive for low Froude numbers. The values of $|C_{P0.1\%}|_{max}$ and $C_{P99.9\%max}$

Table 3 | Values of α, β, γ, δ and the statistical criteria to estimate $P^*_{a\%}$

$P^*_{a\%}$	α	β	γ	δ	R^2	RMSE	MAE	WI
$P^*_{0.1\%}$	–0.0839	0.4781	–1.8210	1.2289	0.756	0.186	0.141	0.994
$P^*_{99.9\%}$	0.3879	8.3165	3.6029	3.2141	0.625	0.160	0.110	0.872

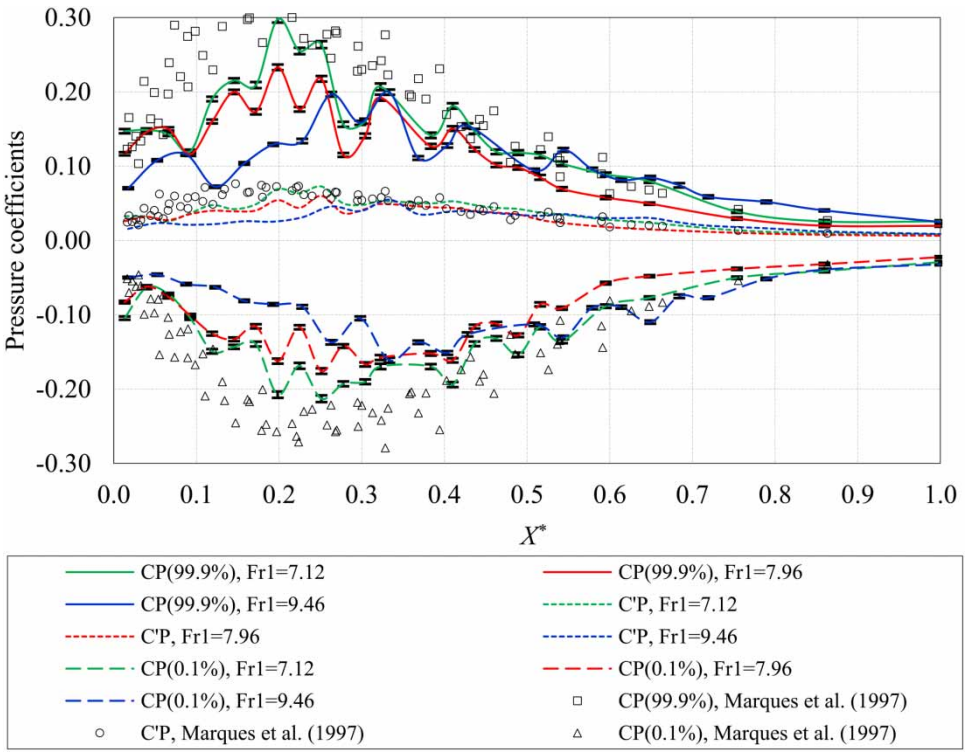

Figure 6 | Longitudinal distribution of $C_{P0.1\%}$, $C_{P99.9\%}$, and C'_P with error bars.

coefficients are necessary to determine the slab thickness and the forces on the slab. According to Table 4, the mean values of C'_{Pmax}, $|C_{P0.1\%}|_{max}$, and $C_{P99.9\%max}$ are approximately 0.06, 0.19, and 0.24, respectively. It should be noted that the maximum negative and positive pressure fluctuation coefficients, namely C_P^- $[(P_{min}-P_m)/V_1^2/2\,g]$ and C_P^+ $[(P_{max}-P_m)/V_1^2/2\,g]$, are usually used instead of $C_{P0.1\%}$ and $C_{P99.9\%}$ coefficients in the literature. Wang *et al.* (1984) proposed a statistical method to define extreme pressures. They stated that pressure values with a low probability, such as 1%, have been applied with a safety factor to estimate extreme conditions. Toso & Bowers (1988) believed that the choice of $|C_P^-|_{max}$ and $C_P{}^+{}_{max}$ coefficients provides a conservative or large pressure loading. According to Table 4, the results of the present study and Marques *et al.* (1997) are slightly less than those obtained by Toso & Bowers (1988).

CONCLUSIONS

Hydraulic jump is one of the most common forms of energy dissipation with the possible damage to the dissipator structures. As a result, it is important to characterize the extreme pressures that may occur as best as possible. In summary, several conclusions are provided from this study, covering the different patterns of pressures within the free hydraulic jumps downstream of an Ogee spillway, equipped with the USBR Type I stilling basin, as follows.

(i) The maximum values of the power spectral density function are close to the frequency of 4 Hz for the free hydraulic jumps. Accordingly, energy dissipation in hydraulic jumps usually has large pressure fluctuations with low frequency. It can be considered as a rapidly varied flow with strong vortices that cause macro-turbulent fluctuations.

(ii) The probability density function (PDF) indicates that the pressure distribution underneath the hydraulic jumps at a given position on the bed of the stilling basin does not follow a normal distribution.

(iii) It is obvious that the pressures corresponding to the lowest cumulative probabilities of occurrence ($P^*_{0.1\%}$) reach lower values, and have negative values around –0.3 up to the approximate $X^* \approx 0.3$. The negative values may indicate zones subject to low pressures and may be related to erosion or cavitation processes. The values of maximum pressures ($P^*_{99.9\%}$) are approximately three times higher than the mean pressure data (P^*_m) at the position around $0.1 \leq X^* \leq 0.3$, justified by the impact of flow on the stilling basin. The uncertainty analysis of the experimental data indicates that the average values of the total standard uncertainty for the multiple variables of P^*_m, $P^*_{0.1\%}$, and $P^*_{99.9\%}$ along the stilling basin are about 1.87, 1.25, and 0.97%, respectively.

(iv) The results indicate that the pressure coefficients increase with decreasing Fr_1. The mean values of C'_{Pmax}, $|C_{P0.1\%}|_{max}$, and $C_{P99.9\%max}$ are approximately 0.06, 0.19, and 0.24, respectively. The results of the present study and Marques *et al.* (1997) for the $|C_{P0.1\%}|_{max}$ and $C_{P99.9\%max}$ coefficients are slightly less than the $|C_P^-|_{max}$ and $C_P{}^+{}_{max}$ coefficients obtained by Toso & Bowers (1988). The uncertainty analysis of the experimental data indicates that the average value of the total standard uncertainty for the multiple variables of $C_{P0.1\%}$ and $C_{P99.9\%}$ along the stilling basin are about 2.35 and 2.64%, respectively.

(v) The results of the current research overlap reasonably well with those found in similar existing works. It should be noted that the hydraulic jump is the multiphase flow phenomenon, with high levels of aeration. Some laboratory equipment fails to provide accurate estimations of experimental variables. The air entrainment in the hydraulic jump makes it difficult for the application of

Table 4 | Maximum values of the dimensionless pressure coefficients

Results	Fr_1	$\lvert C_{P0.1\%}\rvert_{max}$	$\lvert C_P^-\rvert_{max}$	$C_{P99.9\%max}$	$C_P{}^+{}_{max}$	$C'_{P\,max}$
Present study	7.12	0.21	–	0.26	–	0.073
	7.44	0.21	–	0.27	–	0.070
	7.59	0.20	–	0.27	–	0.069
	7.96	0.18	–	0.23	–	0.060
	8.34	0.17	–	0.22	–	0.059
	9.46	0.16	–	0.20	–	0.055
Marques *et al.* (1997)	4.9	0.28	–	0.33	–	0.072
	5.4	0.26	–	0.35	–	0.076
	6.3	0.27	–	0.34	–	0.074
	7.3	0.25	–	0.30	–	0.067
	8.1	0.23	–	0.26	–	0.060
Toso & Bowers (1988)	3.8	–	0.35	–	0.33	–
	4.5	–	0.36	–	0.40	–
	5.1	–	0.32	–	0.40	–
	8.4	–	0.30	–	0.46	–

well-established techniques such as pressure transducers. An extended experimental campaign would improve pressure distribution representation. A better understanding of pressure fluctuations and their distribution may lead to more economical design or greater safety of stilling basins.

(vi) Another aspect of this study is to propose new adjustments to estimate the values of $P^*_{0.1}$ and $P^*_{99.9\%}$ with different cumulative probabilities of occurrence. New second-order rational relationships as a function of X^* were developed, which give more accurate results for $P^*_{0.1}$ and $P^*_{99.9\%}$ estimations.

FUNDING

This research was funded by the University of Tabriz, Iran. The work has been carried out as part of the ongoing PhD dissertation of the first author.

ACKNOWLEDGEMENTS

All co-authors would like to give their gratitude to Prof. Eder Daniel Teixeira, Federal University of Rio Grande do Sul, Porto Alegre, Brazil, for the elaboration of the methodology for analyzing the probability distribution of pressure data, for his expertise, suggestions and valuable comments to improve this manuscript. Also, authors wish to thank the editors and reviewers for their time to review our manuscript and for helping to improve the manuscript.

CONFLICTS OF INTEREST

The authors declare no conflict of interest

REFERENCES

Abdul Khader, M. H. & Elango, K. 1974 Turbulent pressure field beneath a hydraulic jump. *Journal of Hydraulic Research* **12** (4), 469–489.

Alves, A. A. M. 2008 *Caracterização das solicitações hidrodinâmicas em bacias de dissipação por ressalto hidráulico com baixo número de Froude (Characteristics of Hydrodynamic Forces in Dissipation Basins Under Hydraulic Jumps with low Froude Number)*. Master Thesis, Institute for Hydraulic Research. Federal University of Rio Grande do Sul, Porto Alegre (in Portuguese).

American Society of Mechanical Engineers 2013 *ASME PTC 19.1-2013 Test Uncertainty*. The American Society of Mechanical Engineers, New York, NY.

Bennett, N. D., Croke, B. F., Guariso, G., Guillaume, J. H., Hamilton, S. H., Jakeman, A. J., Marsili-Libelli, S., Newham, L. T., Norton, J. P., Perrin, C., Pierce, S. A., Robson, B., Seppelt, R., Voinov, A. A., Fath, B. D. & Andreassian, V. 2013 Characterising performance of environmental models. *Environmental Modelling & Software* **40** (2013), 1–20.

Chanson, H. & Carvalho, R. F. 2015 Hydraulic jumps and stilling basins. In: *Energy Dissipation in Hydraulic Structures* (H. Chanson, ed.). CRC Press, Leiden, The Netherlands. Series: IAHR Monographs, pp. 65–104.

Chiew, Y. M. & Emadzadeh, A. 2017 Experimental investigation of free surface dynamics and pressure fluctuations in a closed-conduit hydraulic jump. In: *E-proceedings of the 37th IAHR World Congress*, August 13–18, 2017, Kuala Lumpur, Malaysia.

Coleman, H. W. & Steele, W. G. 2018 *Experimentation, Validation, and Uncertainty Analysis for Engineers*, 4th edn. John Wiley & Sons, USA.

Dai Prá, M. 2011 *Uma abordagem para determinação das pressões junto ao fundo de dissipadores de energia por ressalto hidráulico (An Approach for Determining Pressures Near the Bottom of the Hydraulic Energy Dissipation Basins)*. PhD Thesis, Institute for Hydraulic Research. Federal University of Rio Grande do Sul, Porto Alegre (in Portuguese).

Dai Prá, M., Priebe, P. S., Teixeira, E. D. & Marques, M. G. 2016 Avaliação das flutuações de pressão em ressalto hidráulico pela dissociação de esforços (Evaluation of pressure fluctuation in hydraulic jump by dissociation of hydraulic forces). *Brazilian Journal of Water Resources (RBRH)* **213** (1), 222–231.

EasyFit professional software 2010 5.5 Mathwave Technologies, Released. Available from: http:/www.mathwave.com.

Endres, L. A. M. 1990 *Contribuição ao Desenvolvimento de um Sistema para Aquisição e Tratamento de Dados de Pressões Instantâneas em Laboratório (Contribution to the Development of A System for the Acquisition and Treatment of Instantaneous Pressure Data in the Laboratory)*. Master Thesis, Institute for Hydraulic Research. Federal University of Rio Grande do Sul, Porto Alegre.

Farhoudi, J., Sadat-Helbar, S. M. & Aziz, N. 2010 Pressure fluctuation around chute blocks of SAF stilling basins. *Journal of Agricultural Science and Technology* **12**, 203–212.

Fiorotto, V. & Caroni, E. 2014 Unsteady seepage applied to lining design in stilling basins. *Journal of Hydraulic Engineering* **140** (7), 1–9.

Fiorotto, V. & Rinaldo, A. 1992 Turbulent pressure fluctuations under hydraulic jumps. *Journal of Hydraulic Research* **30** (4), 499–520.

Hampe, R. F., Steinke Júnior, R., Prá, M. D., Marques, M. G. & Teixeira, E. D. 2020 Extreme pressure forecasting methodology for the hydraulic jump downstream of a low head spillway. *Brazilian Journal of Water Resources (RBRH)* **25** (1), 1–10.

ISO, International Organization for Standardization 1993 *Guide to the Expression of Uncertainty in Measurement*. ISO, Geneva, Switzerland.

Khatsuria, R. M. 2005 *Hydraulics of Spillways and Energy Dissipators*. Marcel Dekker, New York. 649 pp.

Lopardo, R. A., Fattor, C. A., Lopardo, M. C. & Casado, J. M. 2004 *Instantaneous Pressure Field on A Submerged Jump Stilling Basin. Hydraulics of Dams and River Structures*. AA Balkema, London, pp. 133–138.

Macián-Pérez, J. F., García-Bartual, R., Huber, B., Bayon, A. & Vallés-Morán, F. J. 2020 Analysis of the flow in a typified USBR II stilling basin through a numerical and physical modeling approach. *Water Journal* **12** (1), 1–20.

Marques, M. G., Drapeau, J. & Verrette, J. L. 1997 Flutuação de pressão em um ressalto hidráulico (Pressure fluctuation coefficient in a hydraulic jump). *Brazilian Journal of Water Resources (RBRH)* **2** (2), 45–52.

MATLAB 2016 Win 64. Available from: http:/www.mathworks.com.

Neto, E. F. T. & Marques, M. G. 2008 Análise do Campo de Pressões em Ressalto Hidráulico Submergido a Jusante de uma Comporta (Analysis of the pressure field in a submerged hydraulic jump downstream of a sluice gate). *Brazilian Journal of Water Resources (RBRH)* **13** (4), 55–68.

Novakoski, C. K., Hampe, R. F., Conterato, E., Marques, M. G. & Teixeira, E. D. 2017 Longitudinal distribution of extreme pressures in a hydraulic jump downstream of a stepped spillway. *Brazilian Journal of Water Resources (RBRH)* **22** (42), 1–8.

Onitsuka, K., Akiyama, J., Shige-Eda, M., Ozeki, H., Gotoh, S. & Shiraishi, T. 2007 Relationship between pressure fluctuations on the bed wall and free surface fluctuations in weak hydraulic jump. In: *New Trends in Fluid Mechanics Research* (F. G. Zhuang & J. C. Li, eds). Springer, Berlin, Heidelberg, pp. 300–303.

Padulano, R., Fecarotta, O., Del Giudice, G. & Carravetta, A. 2017 Hydraulic design of a USBR type II stilling basin. *Journal of Irrigation and Drainage Engineering* **143** (5), 1–9.

Pei-Qing, L. & Ai-Hua, L. 2007 Model discussion of pressure fluctuations propagation within lining slab joints in stilling basins. *Journal of Hydraulic Engineering* **133** (6), 618–624.

Peterka, A. J. 1984 Stilling basin for high dam and earth dam spillways and large canal structures (basin II). In: *Hydraulic Design of Stilling Basins and Energy Dissipators*, 8th edn (A. J. Peterka, ed.). A Water Resources Technical Publication. Engineering Monograph No. 25. United States Department of the Interior, Bureau of Reclamation. USBR, Denver, CO. US Government Printing Office, USA, pp. 19–30.

Pinheiro, A. 1995 *Acções hidrodinâmicas em soleiras de bacia de dissipação de energia por ressalto hidráulico (Hydrodynamic Actions in Thresholds for Energy Dissipation Basin by Hydraulic Jumps)*. PhD Thesis, Technical University of Lisbon, Portugal (in Portuguese).

Sánchez Bribiesca, J. S. & Vizcaíno, A. C. 1973 Turbulence effects on the lining of stilling basins, ICOLD 11 st Int. In: Congress, Madrid, Spain, Vol. 41.

Souza, P. E. A., Marques, M. G., Trierweiler Neto, E. D. & Teixeira, E. F. 2015 Flutuação de pressão em um ressalto hidráulico de baixa queda e baixo número de Froude a jusante de um vertedouro (Pressure fluctuation in a low-drop and low Froude numbers of hydraulic jump downstream of a spillway). *Brazilian Dam Committee, XXX – Large Dams National Seminar*, Foz do Iguaçu, May 11–13.

Teixeira, E. D. 2003 *Previsão dos valores de pressão junto ao fundo em bacias de dissipação por ressalto hidráulico (Prediction of Pressure Values Close to the Bottom of Dissipation Basins in Hydraulic Jumps)*. Master Thesis, Institute for Hydraulic Research. Federal University of Rio Grande do Sul, Porto Alegre (in Portuguese).

Toso, J. W. & Bowers, C. E. 1988 Extreme pressures in hydraulic-jump stilling basins. *Journal of Hydraulic Engineering* **114** (8), 829–843.

USBR 1987 Spillways. In: *Design of Small Dams*, 3rd edn (A. J. Huber, ed.). A Water Resources Technical Publication. US Department of the Interior, Bureau of Reclamation, Washington, USA. US Government Printing Office, pp. 339–437.

Valero, D., Viti, N. & Gualtieri, C. 2019 Numerical simulation of hydraulic jumps. Part 1: experimental data for modelling performance assessment. *Water Journal* **11** (1), 1–16.

Vasiliev, O. F. & Bukreyev, V. I. 1967 Statistical characteristics of pressure fluctuations in the region of hydraulic jump. *Proc, 12th Congress International Association of Hydraulic Research*, 2, pp. 1–8.

Wang, M., Jiang, C., Xia, B. & Shang, S. 1984 Stochastic analysis of pressure fluctuations beneath hydraulic jump and primary discussion on scale of turbulence. In: *Proc. Fourth IAHR Int. Symposium on Stochastic Hydraulics*, East China Technical University, Nanjing, China, pp. 199–209 (in Chinese).

Yan, Z., Zhou, C. & Lu, S. 2006 Pressure fluctuations beneath spatial hydraulic jumps. *Journal of Hydrodynamics* **18** (6), 723–726.

First received 9 January 2020; accepted in revised form 4 May 2020. Available online 20 May 2020